

SHORT syndrome due to a novel *de novo* mutation in *PRKCE* (Protein Kinase C ϵ) impairing TORC2-dependent AKT activation.

Diana Alcantara¹, Frances Elmslie², Martine Tetreault³, Eric Bareke³, Taila Hartley⁴, Care4Rare Consortium⁴, Jacek Majewski³, Kym Boycott^{4,5}, A. Micheil Innes⁶, David A. Dyment^{4,5,*}, Mark O'Driscoll¹.

Affiliations:

1, Genome Damage and Stability Centre, University of Sussex, Brighton BN1 9RQ, United Kingdom.

2, South West Thames Regional Genetics Service, St. George's, University of London, London SW17 0RE, United Kingdom.

3, McGill University and Genome Quebec Innovation Centre, Montreal, QC H3A 1A4, Canada.

4, Children's Hospital of Eastern Ontario Research Institute, University of Ottawa, Ottawa, ON K1H 8L1, Canada.

5, Department of Genetics, Children's Hospital of Eastern Ontario, Ottawa, ON K1H 8L1, Canada.

6, Department of Medical Genetics, Alberta Children's Hospital Research Institute for Child and Maternal Health, University of Calgary, Calgary, AB T2N, Canada.

Correspondence to:

*Dr. David Dyment, Children's Hospital of Eastern Ontario Research Institute, 401 Smyth Road, Ottawa, Ontario, Canada; ddyment@cheo.on.ca

Abstract

SHORT syndrome is a rare, recognizable syndrome resulting from heterozygous mutations in *PIK3R1* encoding a regulatory subunit of phosphoinositide-3-kinase (PI3K). The condition is characterized by short stature, intrauterine growth restriction, lipodystrophy and a facial gestalt involving a triangular face, deep set eyes, low hanging columella and small chin. *PIK3R1* mutations in SHORT result in reduced signaling through the PI3K-AKT-mTOR pathway. We performed whole exome sequencing for an individual with clinical features of SHORT syndrome but negative for *PIK3R1* mutation and her parents. A novel candidate variant was identified, expressed and examined using *ex vivo* kinase assay. AKT-mTOR pathway function was assessed using phospho-specific antibodies with patient lymphoblasts and following ectopic expression of the mutant in HEK293 cells. A rare *de novo* variant in *PRKCE* encoding PKC ϵ was identified. Kinase analysis showed it to be partial loss-of-function. Whilst interaction with PDK1 and the mTORC2 complex component SIN1 was preserved in the mutant PKC ϵ , it bound to SIN1 with a higher affinity than wild-type PKC ϵ and the dynamics of mTORC2-dependent priming of mutant PKC ϵ was altered. Further, mutant PKC ϵ caused impaired mTORC2-dependent pAKT-S473 following rapamycin treatment. Reduced pFOXO1-S256 and pS6-S240/244 levels were also observed in the patient LCLs. To date, mutations in *PIK3R1* causing impaired PI3K-dependent AKT activation are the only known cause of SHORT syndrome. We identify a SHORT syndrome child with a novel partial loss-of-function defect in PKC ϵ . This variant causes impaired AKT activation via compromised mTORC2 complex function.

Introduction

SHORT syndrome is a rare malformation syndrome (MIM: 269880) with less than 40 confirmed cases reported in the literature (1, 2). The acronym for SHORT syndrome is defined as **S**hort stature, **H**yperextensibility/Inguinal Hernias, **O**cular depression, **R**ieger anomaly and **T**eething delay (1, 3). A recent appraisal of the literature of confirmed cases has highlighted the most common features of this syndrome and this includes intrauterine growth restriction, lipoatrophy and a facial gestalt that is near universal among those with SHORT syndrome (1). The facial features comprise a broad forehead, deep set eyes, low-hanging columella, prominent ears and a triangular appearance to the face and a chin that may be dimpled (1). Other prevalent characteristics include insulin resistance, short stature and a low body mass index (1). While there are common features, close to half (48%) of the individuals with SHORT syndrome will have 3 or less of the features described in the acronym (1).

Mutations in *PIK3R1* were identified as the cause of SHORT syndrome by ourselves and other research groups (4-6). The mutations typically reside in the regulatory domain of *PIK3R1* that encodes the p85 α subunit of phosphoinositide-3-kinase (PI3K) and includes a recurrent substitution, R649W. This p85 α subunit acts to regulate the catalytic subunit (p110) of PI3K, and when p85 α is phosphorylated, it will uncouple from the p110 subunit. Consequently, p110 is available to catalyze phosphatidylinositol (4,5) bisphosphate to phosphatidylinositol (3,4,5) triphosphate and thereby initiate downstream phosphorylation of targets to promote cellular growth via the PI3K-AKT-mTOR pathway. Individuals with mutation in the p85 α sequence show reduced signaling via the PI3K-AKT-mTOR network demonstrated by diminished phosphorylation of downstream targets such as AKT, S6K and S6 (2, 4-6).

Here we present the case of a 13 year old girl with the clinical characteristics of SHORT syndrome and a *de novo* mutation in *PRKCE*. The mutation results in impaired activation of AKT specifically via the mTORC2 complex-dependent branch of this pathway.

Results

The proband was born to a 28 year old mother after a pregnancy complicated by nonimmune fetal hydrops detected at 20 weeks gestation. A pleural shunt was inserted and the hydrops was found to have resolved completely by 37 weeks gestation. Her mother was referred to the genetics service, but other than a karyotype, no genetic testing was undertaken during the pregnancy. There was no intrauterine growth restriction described during the pregnancy. She was born by elective Caesarean section at 38 weeks and weighed 2500 grams ($Z = -1.7$ SD) and with a head circumference of 33 cm ($Z = -0.7$ SD). She was reviewed by a geneticist in the neonatal period who noted that she had a prominent nose, a high nasal bridge and a small chin (Figure 1A-C). She had an unusual distribution of fat, and her abdomen had a prune belly-like appearance. Soon after birth, she developed dusky episodes for which she was investigated. An echocardiogram demonstrated mild mitral regurgitation and mild left pulmonary artery branch stenosis which resolved completely by the age of 4 years.

She was reviewed regularly in the genetics clinic. Over time her scalp hair continued to be sparse and she had hypodontia. She had pale, translucent skin with prominent vasculature and a paucity of body fat. When reviewed at age 13 she was developmentally age appropriate and doing well in school. There was no past history of any delays in meeting developmental milestones (speech, fine and gross motor). She had a history of frequent bouts of otitis media and recurrent urinary tract infections. An abdominal scan showed scarring of one kidney. There was no history of ophthalmological concerns (no anterior chamber defects or otherwise) or inguinal hernias. On examination at age 13 she had a height of 147.8 cm ($Z = -1.32$ SD), weight of 32.54kg ($Z = -2$ SD) and a BMI of 15.06 ($Z = -1.9$). She had a triangular face and a broad forehead (Figure 1D-E). Palpebral fissures were deep set and she had a prominent nasal root. Her nose was long with an overhanging columella. Mouth and chin were normally shaped with no dimple. Ears were prominent but normally positioned and with normal structure. There were normal nails, digits and creases to hands and feet. She had persistent primary dentition, and was lacking eight adult teeth. Extremities and her face showed a paucity of fat and prominent vasculature. She had a pectus excavatum and a slender body habitus.

A diagnosis of partial lipodystrophy was initially considered, but clinical testing for mutations in *LMNA* was normal and she had normal C3 nephritic factor, fasting triglycerides, cholesterol and glucose. Later, the connective tissue abnormalities led to a consideration of Ehlers-Danlos syndrome type IV. A skin biopsy showed irregular collagen fibrils but *COL3A1* sequencing and MLPA was negative for a mutation. A diagnosis of SHORT syndrome was then considered on clinical grounds and the patient referred for testing of *PIK3R1*.

Given the strong clinical suspicion of SHORT syndrome, targeted Sanger sequencing of *PIK3R1* was performed with no mutations identified. After WES, no obvious pathogenic variants or small deletions/duplications in *PIK3R1* or in other known genes were identified that could explain the individual's presentation (Supplementary Information). However, a *de novo* variant in *PRKCE* was highlighted based on its rarity and the kinase function of its product, Protein Kinase C family member epsilon (PKC ϵ). The Protein Kinase C family of serine/threonine protein kinases are organized into three classes; conventional (cPKC: α, β, γ), novel (nPKC: $\delta, \epsilon, \eta, \theta$) and atypical (aPKC: ζ, ι). Collectively, they influence a complex array of diverse cellular functions including cell proliferation, survival, apoptosis and migration (7, 8). Importantly in the context of SHORT syndrome, PKC ϵ functions in controlling cell proliferation via the AKT-mTOR pathway (9-12). The variant identified was NM_005400.2 (*PRKCE*): exon 13:c.1795G>A: p. E599K, altering a highly conserved residue within the kinase domain of PKC ϵ (Figure 2A & Supplementary Table 2). This variant was not present in ExAC, gnomAD or ClinVar, although it was reported in a single cutaneous melanoma sample (TCG-ER-1198) in COSMIC and cBioPortal. Multiple pathogenicity prediction algorithms predict the variant to be damaging (Supplementary Table 1). Sanger sequencing of the patient and her parents was performed and confirmed that the variant was present and was *de novo*.

To determine the variants' impact on the enzyme activity, E599K was introduced into a *PRKCE*-containing mammalian expression vector (MYC-FLAG-pCMV6) by site-directed mutagenesis and expressed in HEK293 cells. Following immunoprecipitation via the FLAG-tag and elution using FLAG peptide the resultant PKC ϵ -specific eluate was tested for its kinase activity using the PepTag PKC Kinase Activity platform (Figure 2B). The kinase

activity of E559K was approximately 50% that of wild-type (WT) (Figure 2C). K437M is an ATP binding defective “kinase dead” (KD) and served as a negative control. E599K retained some activity above the kinase-dead control. Therefore, these results demonstrate E599K to be a partial loss-of-function mutant. Furthermore, combining WT and E599K in the kinase assay did not demonstrate additivity, suggesting a degree of dominant negativity is also a feature of E599K (Figure 2D)

The PKC family resides in the AGC branch of the human kinome. AGC kinases, which include AKT, share a similar mechanism of activation involving priming through phosphorylation by other kinases of conserved priming sites within (activation loop motif, turn motif) and C-terminal to (hydrophobic motif) their kinase domain (13, 14). For PKC ϵ , T566 represents the activation loop, T710 the turn motif, and S729 the hydrophobic motif (Figure 2A). The kinases involved in PKC ϵ priming are PDK1 (T566) and the mTORC2 complex (T710, S729). Primed PKC ϵ can exist in an auto-inhibited latent state through occupation of its substrate binding pocket by its pseudosubstrate domain (Figure 3A). This dynamic latent stage protects the phosphorylated priming sites from dephosphorylation and facilitates rapid full activation upon subsequent substrate-mediated dynamic allosteric conformational changes within the active site. Unprimed (unphosphorylated) PKC ϵ is inactive. We examined priming of S729 (mTORC2-dependent) in patient LCLs using the only commercially available phospho-specific priming antibody for PKC ϵ ; that of phospho-S729 (pPKC ϵ -S729). We found reduced levels of pPKC ϵ -S729 in PKC ϵ SHORT syndrome LCLs compared to those of the unaffected parent (Figure 3B). We next examined the ability of native PKC ϵ to interact with the mTORC2 priming kinase via immunoprecipitation with the mTORC2 complex subunit SIN1 (15). Interestingly, we observed enhanced affinity of PKC ϵ from the SHORT syndrome LCLs for SIN1, compared to parental LCLs (Figure 3C). Similarly, using ectopically expressed wild-type (WT) and E599K, we observed enhanced SIN1 affinity of the mutant PKC ϵ (Figure 3D). WT and E599K bound with grossly comparable affinity to the other priming kinase, PDK1, under these conditions (Figure 3E).

We found that priming of S729 (mTORC2-dependent) following ectopic expression in HEK293 cells was comparable between wild-type (WT) and E599K (Figure 3F). We similarly found pPKC ϵ -S729 levels comparable between E599K, wild-type (WT) and a

constitutively active (CA; A159E) PKC ϵ , in contrast to kinase-dead (KD) ATP-binding mutant, in these cells (Figure 3G). It is known that monitoring the dynamics of phosphorylation on PKC family members is challenging as these are generally constitutively phosphorylated in cell culture (16). Parker and colleagues have developed a strategy to overcome this constitutive phosphorylation to enable the study of priming dynamics by altering the conserved active site K residue that contacts the α - β phosphates of ATP (14). This K437M kinase-dead variant is unprimed (unphosphorylated) at all priming motifs (Figure 3G)(14). Interestingly, we found that when E599K was engineered *in cis* into a K437M containing protein, this doubly mutant PKC ϵ remained primed by phosphorylation at S729 (Figure 3H). This was in contrast to K437M alone or *in cis* with the constitutively active (CA) A159E variant (Figure 3H). This suggests restricted allosteric flexibility within the active site of PKC ϵ containing E599K. This exact phenotype is associated with markedly reduced kinase activity in other kinase-site variants such as D532A and D532N (14). Therefore, one possible explanation for the reduction in kinase activity we observed in E599K (Figure 2B-D), is that the catalytic kinase domain more stably adopts a less flexible allosteric conformation reminiscent of the latent form of PKC ϵ (Figure 3A).

AKT is also a member of the AGC kinase family and similar to PKCs requires priming phosphorylation for optimal activity (14). In fact, phosphorylation of these priming residues are commonly used to probe AKT activity status. The activation loop motif residue of AKT is T308 (PDK1-dependent) and the hydrophobic motif is S473 (mTORC2-dependent). PKC ϵ has been implicated in AKT activation via the mTORC2 complex (14). Rapamycin (RapM) inhibits mTORC1 complex specifically, but can be used to monitor mTORC2 activity (14, 16). Using LCLs from an unaffected parent and the PKC ϵ -SHORT syndrome individual, we monitored the phospho-status of AKT on S473 (mTORC2 phospho-site) and T308 (PDK1 phospho-site) following treatment with RapM to leverage signaling through mTORC2. We found reduced RapM-dependent pAKT-S473 in PKC ϵ -SHORT syndrome LCLs, compared to the parental cells (Figure 4A). This was in contrast to phosphorylation of the PDK1-dependent T308 site in AKT, which exhibited similar kinetics between parental and PKC ϵ -SHORT syndrome LCLs under these conditions (Figure 4A). These findings indicate reduced mTORC2-dependent phosphorylation and consequently full activation of AKT in PKC ϵ -SHORT syndrome LCLs. Consequently, we also observed reduced AKT-

dependent FOXO1 phosphorylation (pFOXO1-S256) in PKC ϵ SHORT syndrome LCLs compared to parental LCLs under these conditions (Figure 4A).

SHORT syndrome caused by mutant *PIK3R1* (p85 α) has previously been shown to be associated with reduced phospho-priming of AKT (2, 5, 6). Consistent with this we also demonstrated incomplete AKT priming phosphorylation in p85 α -SHORT syndrome LCLs following RapM treatment (Figure 4B). In this instance PDK1-dependent phospho-priming was clearly reduced as evidenced by the lower levels of pAKT-T308 in p85 α -SHORT syndrome LCLs compared to wild-type (WT) LCLs under these conditions. A positive feedback loop between AKT and mTORC2 has recently been described and which may be reflected in the somewhat lower RapM-induced pAKT-S473 levels seen in p85 α -SHORT syndrome LCLs compared to WT here (Figure 4B) (14, 17). Reduced AKT-dependent FOXO1 phosphorylation (pFOXO1-S256) was also observed in p85 α -SHORT syndrome LCLs compared to WT under these conditions (Figure 4B).

To demonstrate impaired mTORC2-dependent AKT activation is directly caused by E599K PKC ϵ we modeled its impact upon AKT activation following over-expression in HEK293 cells and treatment with RapM. Reduced pAKT-S473 was observed following E599K over-expression, similar to K437M kinase-dead (KD), and consistent with impaired AKT function under these conditions (Figure 4C). To be optimally active AKT requires phosphorylation of all of its priming motifs. Our findings show that E599K PKC ϵ can impair AKT priming similarly to p85 α -defects, but in this instance, the impairment occurs mainly through the established PKC ϵ -mTORC2 route.

Phorbol 12-myristated 13-acetate (PMA) can activate PKC ϵ by binding its pseudosubstrate domain and relieving auto-inhibition. We examined AKT-mTORC1 activity following treatment with PMA in PKC ϵ -SHORT syndrome LCLs under low serum (LS) conditions. Whilst we did not observe a clear increase in phospho-S6 (S240, S244) following PMA in parental LCLs, the level of pS6 was markedly reduced under these conditions specifically in PKC ϵ SHORT syndrome LCLs (Figure 4D). These results are indicative of reduced activity

through the AKT-mTOR-S6K-S6 pathway in PKC ϵ -SHORT syndrome, as has previously also been described in p85 α -SHORT syndrome (Figure 5).

Discussion

We have presented a child with the clinical and cellular signaling deficits in keeping with SHORT syndrome, though due to a novel, dominant, heterozygous mutation in *PRKCE* versus *PIK3RI*. The patient's facial features were similar to that of classical SHORT syndrome, in particular the shape of the forehead, nose and the deep-set eyes. The lack of family history, normal development, the history of hypodontia and her lipodystrophy were also typical SHORT syndrome clinical features. At the cellular level, the diminished phosphorylation of AKT and other downstream targets of the AKT-mTOR network (Figure 4) is also seen in SHORT syndrome (4, 5). Given these broad similarities we would state that heterozygous mutation in *PRKCE* represent a second SHORT syndrome disease gene. However, we would differentiate this presentation from the "Short syndrome type 2" recently described by Pronterra *et al.* (18). In their report the affected child carried biallelic mutations in *IGFRI* as well as central nervous system malformations, global developmental delays, microcephaly and elevated triglycerides, none of which would be expected in the *PIK3RI*- or *PRKCE*-related forms of SHORT syndrome.

We recognize that the individual presented here does not have all the cardinal manifestations described in the SHORT syndrome acronym, though this is not unexpected as only half of individuals with SHORT syndrome, and with confirmed mutations in *PIK3RI*, have 4 or more of the hallmark features (1). The individual presented here was less than average for height, but only mildly so, and with a lower BMI but within the normal range (Z scores of height and BMI were -1.2 and -1.9 respectively). Other SHORT syndrome features were also absent such as anterior chamber deficits (Rieger anomaly) and inguinal hernias, but these are present in only a minority (<30%) of those with SHORT syndrome (1). Insulin resistance is commonly seen in SHORT syndrome but it was absent in our relatively young patient although an oral glucose tolerance test had not been performed at the time of the manuscript preparation. Of note, those with heterozygous, pathogenic mutations in the same pathway, but in *AKT2* (OMIM 164731), do show insulin resistance though starting in the third-fourth

decade of life (19) and those with *PIK3R1*-related SHORT syndrome develop overt diabetes in the second decade or older (20, 21).

A pathogenic role for PKC ϵ has been known for several types of cancers as it is able to promote proliferation and inhibit apoptosis (22, 23). Constitutively active PKC ϵ has been found in small cell lung cancer (24) and its over-expression in fibroblasts (25, 26) and epithelial cells of the colon (27) has been associated with tumor formation with PKC ϵ being described as an oncogene (28). Over 150 somatic mutations, mostly substitutions, in *PRKCE* have been described in tumors (29). Recently, a comprehensive functional evaluation of multiple cancer-associated PKC mutations, including those of PKC ϵ , surprisingly found none to be activating, with most being loss-of-function (30). The PKC ϵ variant we describe here in SHORT syndrome (E599K) appears to be partial loss-of-function for kinase activity.

Although E599K, as noted earlier, has been described in a single instance of cutaneous melanoma, this sample appears genomically highly complex and also contains known oncogenic hyper-activating variants in *BRAF* and *AKT1* (see http://www.cbioportal.org/case.do?cancer_study_id=skcm_tcg&case_id=TCGA-ER-A198)

Nonetheless, we provide the first functional characterization of PKC ϵ E599K and show it impairs AKT activation in the constitutional context of SHORT syndrome. Our work highlights the synergistic benefit of combining genetic analysis with molecular-cellular characterization of suspect pathogenic variants.

Outside of cancer, defects in PKC family members are very rare. To date, only mutations in *PRKCD* encoding PKC δ have been identified in a human congenital disease: Systemic Lupus Erythematosus with defective B cell apoptosis and hyper-proliferation (31). While there are no reported loss-of-function *PRKCE* mutations associated with human disease, homozygous loss-of-function mouse models of Pkc ϵ show phenotypic similarities to our patient. Mice homozygous for a disruption of *Prkce* were smaller by 10-15% and also show less overall adipose tissue with age (32) though this has not been seen in all models (33). Nonetheless, reduced Pkc ϵ function has also been found to impair adipogenic differentiation in mouse preadipocyte cell culture systems (34, 35). *Prkce*^{-/-} mice also show a propensity to gram negative infections as macrophages were less sensitive to exposure to lipopolysaccharides (32). Another knockout mouse was employed to investigate the role of PKC ϵ in insulin

metabolism (33). These *Prkce*^{-/-} mice showed an improved ability to maintain glucose levels in fasting conditions compared to their wild-type littermates (33). *Akt* deficient mice are smaller and also lack the diabetic phenotype, comparable to the *Prkce*^{-/-} mice (36). Double knockout mice deficient in *Akt1* and *Akt2* die shortly after birth, but show impaired adipogenesis and significant growth restriction (37). This is in marked contrast to *Pik3r1* deficient mice as they have striking evidence of insulin resistance as well as small size and lipoatrophy (38).

In closing, we identify and characterize a novel genetic defect in SHORT syndrome. We show that the partial loss of kinase activity of PKC ϵ E599K is associated with reduced mTORC2-dependent phospho-priming and activation of AKT. Whilst impaired AKT activation has previously been described as a pathomechanism underlying p85 α SHORT syndrome, we show that *de novo* constitutional mutation in *PRKCE* (PKC ϵ) is similarly associated with compromised AKT-mTOR activation, albeit mainly via impaired mTORC2 signaling (Figure 5). Our findings represent the first example of a constitutional mutation in *PRKCE* (PKC ϵ) in human disease.

Materials and Methods

The Care4Rare Canada Consortium is a collaborative research project with the goal of identifying genetic mutations for rare childhood diseases. Institutional research ethics board (Children's Hospital of Eastern Ontario) approval of the study design was obtained and free and informed consent was obtained from the study subject prior to enrollment.

Sequencing

Exome capture and high-throughput sequencing of genomic DNA was performed on the proband and parents at the Genome Quebec Innovation Center (Montreal, Canada). Target enrichment for the samples was performed using the Agilent SureSelect 50 Mb (V5) All Exon Kit. Sequencing (Illumina HiSeq) generated >14 Gbp of 100 base pair, paired-end reads per sample. Read alignment, variant calling and annotation were done as for previous Care4Rare projects with a pipeline based on BWA(39), Picard (<http://picard.sourceforge.net/>), ANNOVAR and custom annotation scripts. Reads were aligned to hg19 with BWA 0.5.9, and indel realignment was done using the GATK(40). Duplicate reads were then marked using Picard and excluded from downstream analyses. We assessed coverage of consensus coding sequence (CCDS) bases using the GATK, which showed that all samples had >95% of CCDS bases covered by at least 20 reads. Single nucleotide variants (SNVs) and short insertions and deletions (indels) were called using SAMtools pileup with the extended base alignment quality (BAQ) adjustment (-E), and were then quality filtered to require at least 20% of reads supporting the variant call. Variants were annotated using both ANNOVAR and custom scripts to identify whether they affected protein coding sequence, *in silico* pathogenicity and conservation predictions, and whether they had previously been seen in dbSNP138, the 1000 genomes dataset (2012/04 release), the 6500 NHLBI exomes (Exome Variant Server, NHLBI GO Exome Sequencing Project (ESP), Seattle, WA, data downloaded; 09/2015), the Exome Aggregation Consortium, or in approximately 2000 exomes previously sequenced at the McGill University and Genome Quebec Innovation Centre. Variants were disregarded if they were present at a frequency higher than 5%. Sanger sequencing of the patient and her parents were also performed for the

candidate variant(s). A summary of the variant filtering is presented as Supplementary Table 1.

Cell Lines

HEK293 cells were grown at 37°C with 5% CO₂ in DMEM with 10% foetal calf serum (FCS), L-GLN and antibiotics (Pen-Strep). Patient EBV transformed lymphoblastoid cells (LCLs) were grown in RPMI1640 supplemented with 15% FCS, L-GLN and antibiotics (Pen-Strep).

Antibodies and chemicals

Anti-pPKC ϵ -S729 (sc-12355) and anti- β -tubulin (sc-9104) were from Santa Cruz Biotechnology. Anti-PKC ϵ [EIP1482(2)] was from Abcam. Mouse monoclonal anti-FLAG® M2 (F3165) was from SIGMA-ALDRICH. Antibodies against pan-AKT (4691), pAKT- S473 (4060), pAKT- T308 (2965), S6 (2217), pS6-S240/244 (2215), FOXO1 (2880), pFOXO1-S256 (9461), SIN1 (12860) and PDK1 (3062) were from Cell Signaling Technology. Rapamycin was obtained from Tocris Bioscience and Phorbol 12-myristated 13-acetate (PMA) P8139 from SIGMA-ALDRICH.

Plasmids, site-directed mutagenesis, transfection and immunoprecipitation

PRKCE (MYC-DDK-tagged) in pCMV6 TrueORF Gold encoding human PKC ϵ (NM_005400) was obtained from Origene (Cat# RC217702). Sequence variants were introduced here using the QuikChange® Site-Directed Mutagenesis Kit (Cat# 200518) from Agilent Technologies (Stratagene) according to manufacturers' instructions. The primer pairs are:

E599K Forward: 5' GGGTGCTGATGTACAAGATGATGGCTGGAC 3'
 Reverse: 5' GTCCAGCCATCATCTTGTACATCAGCACCC 3'

K437M Forward: 5' GAAGTATATGCTGTGATGGTCTTAAAGAAGGACG 3'
 Reverse: 5' CGTCCTTCTTTAAGACCATCACAGCATATACTTC 3'

T566A Forward: 5' GTGACGACCACCGCGTTCTGTGGGAC 3'
Reverse: 5' GTCCCACAGAACGCGGTGGTCGTCAC 3'

HEK293 cells were transfected using calcium phosphate technique with 5µg of plasmid DNA, 2M CaCl₂ and HBS (NaCl, Na₂HPO₄, HEPES pH7.5), harvested 48hrs later and the pellet resuspended in extraction buffer (50mM Tris.HCl pH7.5, 150mM NaCl, 2mM EDTA, 2mM EGTA, 50mM NaF, 25mM β-glycerolphosphate, 0.1mM Na-orthovanadate, 0.2% Triton-X100, 0.3% IGEPAL, protease inhibitor cocktail (Roche)). 300µg of extract was subsequently used for immunoprecipitation with Anti-FLAG® M2 Affinity Gel (A2220 from SIGMA-ALDRICH).

PepTag *ex vivo* Kinase assay

Immunoprecipitated (via FLAG-tag) PKCε was eluted from the affinity gel using 3X FLAG® Peptide (F4799 from SIGMA-ALDRICH) and used in the non-radioactive PepTag® assay for PKC kinase activity (V5330 from Promega), according to the manufacturers' instructions. The PKC-specific fluorescent peptide substrate C1 peptide used is P-L-S-R-T-L-S-V-A-A-K.

Acknowledgements

The authors would like to acknowledge the patient and her family.

Funding

This work was performed under the Care4Rare Canada Consortium funded by Genome Canada, the Canadian Institutes of Health Research, the Ontario Genomics Institute, Ontario Research Fund, Genome Quebec, and Children's Hospital of Eastern Ontario Foundation. Programme funding was also provided by Cancer Research UK (C24110/A15394).

Competing interests

The authors declare no conflict of interest.

References/

- 1 Avila, M., Dymment, D.A., Sagen, J.V., St-Onge, J., Moog, U., Chung, B.H., Mansour, S., Albanese, A., Garcia, S., Ortiz Martin, D. *et al.* (2016) Clinical reappraisal of SHORT syndrome with PIK3R1 mutations: towards recommendation for molecular testing and management. *Clin Genet.* **89**, 501-506.
- 2 Huang-Doran, I., Tomlinson, P., Payne, F., Gast, A., Sleight, A., Bottomley, W., Harris, J., Daly, A., Rocha, N., Rudge, S. *et al.* (2016) Insulin resistance uncoupled from dyslipidemia due to C-terminal PIK3R1 mutations. *JCI Insight*, **1**, e88766.
- 3 Gorlin, R.J., Cervenka, J., Moller, K., Horrobin, M. and Witkop, C.J. (1975) Malformation syndromes. A selected miscellany. *Birth Defects Orig Artic Ser*, **11**, 39-50.
- 4 Dymment, D.A., Smith, A.C., Alcantara, D., Schwartzentruber, J.A., Basel-Vanagaite, L., Curry, C.J., Temple, I.K., Reardon, W., Mansour, S., Haq, M.R. *et al.* (2013) Mutations in PIK3R1 Cause SHORT Syndrome. *Am J Hum Genet*, **93**, 158-166.
- 5 Chudasama, K.K., Winnay, J., Johansson, S., Claudi, T., König, R., Haldorsen, I., Johansson, B., Woo, J.R., Aarskog, D., Sagen, J.V. *et al.* (2013) SHORT syndrome with partial lipodystrophy due to impaired phosphatidylinositol 3 kinase signaling. *Am J Hum Genet*, **93**, 150-157.
- 6 Thauvin-Robinet, C., Auclair, M., Duplomb, L., Caron-Debarle, M., Avila, M., St-Onge, J., Le Merrer, M., Le Luyer, B., Héron, D., Mathieu-Dramard, M. *et al.* (2013) PIK3R1 mutations cause syndromic insulin resistance with lipodystrophy. *Am J Hum Genet*, **93**, 141-149.
- 7 Dempsey, E.C., Newton, A.C., Mochly-Rosen, D., Fields, A.P., Reyland, M.E., Insel, P.A. and Messing, R.O. (2000) Protein kinase C isozymes and the regulation of diverse cell responses. *Am J Physiol Lung Cell Mol Physiol*, **279**, L429-438.
- 8 Rosse, C., Linch, M., Kermorgant, S., Cameron, A.J., Boeckeler, K. and Parker, P.J. (2010) PKC and the control of localized signal dynamics. *Nat Rev Mol Cell Biol*, **11**, 103-112.

- 9 Cameron, A.J., Linch, M.D., Saurin, A.T., Escribano, C. and Parker, P.J. (2011) mTORC2 targets AGC kinases through Sin1-dependent recruitment. *Biochem J*, **439**, 287-297.
- 10 Ikenoue, T., Inoki, K., Yang, Q., Zhou, X. and Guan, K.L. (2008) Essential function of TORC2 in PKC and Akt turn motif phosphorylation, maturation and signalling. *EMBO J*, **27**, 1919-1931.
- 11 Moschella, P.C., McKillop, J., Pleasant, D.L., Harston, R.K., Balasubramanian, S. and Kuppuswamy, D. (2013) mTOR complex 2 mediates Akt phosphorylation that requires PKC ϵ in adult cardiac muscle cells. *Cell Signal*, **25**, 1904-1912.
- 12 Huang, C., Ma, W.Y. and Dong, Z. (1998) Potentiation of insulin-induced phosphatidylinositol-3 kinase activity by phorbol ester is mediated by protein kinase C epsilon. *Cell Signal*, **10**, 185-190.
- 13 Cameron, A.J. and Parker, P.J. (2010) Protein kinase C - a family of protein kinases, allosteric effectors or both? *Adv Enzyme Regul*, **50**, 169-177.
- 14 Cameron, A.J., Escribano, C., Saurin, A.T., Kostelecky, B. and Parker, P.J. (2009) PKC maturation is promoted by nucleotide pocket occupation independently of intrinsic kinase activity. *Nat Struct Mol Biol*, **16**, 624-630.
- 15 Bhaskar, P.T. and Hay, N. (2007) The two TORCs and Akt. *Dev Cell*, **12**, 487-502.
- 16 Wan, X., Harkavy, B., Shen, N., Grohar, P. and Helman, L.J. (2006) Rapamycin induces feedback activation of Akt signaling through an IGF-1R-dependent mechanism. *Oncogene*, **26**, 1932-1940.
- 17 Yang, G., Murashige, Danielle S., Humphrey, Sean J. and James, David E. (2015) A Positive Feedback Loop between Akt and mTORC2 via SIN1 Phosphorylation. *Cell Reports*, **12**, 937-943.
- 18 Prontera, P., Micale, L., Verrotti, A., Napolioni, V., Stangoni, G. and Merla, G. (2015) A New Homozygous IGF1R Variant Defines a Clinically Recognizable Incomplete Dominant form of SHORT Syndrome. *Hum Mutat*.
- 19 George, S., Rochford, J.J., Wolfrum, C., Gray, S.L., Schinner, S., Wilson, J.C., Soos, M.A., Murgatroyd, P.R., Williams, R.M., Acerini, C.L. *et al.* (2004) A family with severe insulin resistance and diabetes due to a mutation in AKT2. *Science*, **304**, 1325-1328.
- 20 Schwingshandl, J., Mache, C.J., Rath, K. and Borkenstein, M.H. (1993) SHORT syndrome and insulin resistance. *Am J Med Genet*, **47**, 907-909.

- 21 Aarskog, D., Ose, L., Pande, H. and Eide, N. (1983) Autosomal dominant partial lipodystrophy associated with Rieger anomaly, short stature, and insulinopenic diabetes. *Am J Med Genet*, **15**, 29-38.
- 22 Jain, K. and Basu, A. (2014) Protein Kinase C-ε Promotes EMT in Breast Cancer. *Breast Cancer (Auckl)*, **8**, 61-67.
- 23 Jain, K. and Basu, A. (2014) The Multifunctional Protein Kinase C-ε in Cancer Development and Progression. *Cancers (Basel)*, **6**, 860-878.
- 24 Baxter, G., Oto, E., Daniel-Issakani, S. and Strulovici, B. (1992) Constitutive presence of a catalytic fragment of protein kinase C epsilon in a small cell lung carcinoma cell line. *J Biol Chem*, **267**, 1910-1917.
- 25 Mischak, H., Goodnight, J.A., Kolch, W., Martiny-Baron, G., Schaechtle, C., Kazanietz, M.G., Blumberg, P.M., Pierce, J.H. and Mushinski, J.F. (1993) Overexpression of protein kinase C-delta and -epsilon in NIH 3T3 cells induces opposite effects on growth, morphology, anchorage dependence, and tumorigenicity. *J Biol Chem*, **268**, 6090-6096.
- 26 Mischak, H., Goodnight, J., Henderson, D.W., Osada, S., Ohno, S. and Mushinski, J.F. (1993) Unique expression pattern of protein kinase C-theta: high mRNA levels in normal mouse testes and in T-lymphocytic cells and neoplasms. *FEBS Lett*, **326**, 51-55.
- 27 Perletti, G.P., Folini, M., Lin, H.C., Mischak, H., Piccinini, F. and Tashjian, A.H. (1996) Overexpression of protein kinase C epsilon is oncogenic in rat colonic epithelial cells. *Oncogene*, **12**, 847-854.
- 28 Gorin, M.A. and Pan, Q. (2009) Protein kinase C epsilon: an oncogene and emerging tumor biomarker. *Mol Cancer*, **8**, 9.
- 29 Forbes, S.A., Beare, D., Boutselakis, H., Bamford, S., Bindal, N., Tate, J., Cole, C.G., Ward, S., Dawson, E., Ponting, L. *et al.* (2017) COSMIC: somatic cancer genetics at high-resolution. *Nucleic Acids Res*, **45**, D777-D783.
- 30 Antal, C.E., Hudson, A.M., Kang, E., Zanca, C., Wirth, C., Stephenson, N.L., Trotter, E.W., Gallegos, L.L., Miller, C.J., Furnari, F.B. *et al.* (2015) Cancer-associated protein kinase C mutations reveal kinase's role as tumor suppressor. *Cell*, **160**, 489-502.
- 31 Belot, A., Kasher, P.R., Trotter, E.W., Foray, A.P., Debaud, A.L., Rice, G.I., Szykiewicz, M., Zabet, M.T., Rouvet, I., Bhaskar, S.S. *et al.* (2013) Protein kinase cδ deficiency causes mendelian systemic lupus erythematosus with B cell-defective apoptosis and hyperproliferation. *Arthritis Rheum*, **65**, 2161-2171.

- 32 Castrillo, A., Pennington, D.J., Otto, F., Parker, P.J., Owen, M.J. and Boscá, L. (2001) Protein kinase Cepsilon is required for macrophage activation and defense against bacterial infection. *J Exp Med*, **194**, 1231-1242.
- 33 Raddatz, K., Frangioudakis, G., Diakanastasis, B., Liao, B.M., Leitges, M. and Schmitz-Peiffer, C. (2012) Deletion of protein kinase Cε in mice has limited effects on liver metabolite levels but alters fasting ketogenesis and gluconeogenesis. *Diabetologia*, **55**, 2789-2793.
- 34 Webb, P.R., Doyle, C. and Anderson, N.G. (2003) Protein kinase C-epsilon promotes adipogenic commitment and is essential for terminal differentiation of 3T3-F442A preadipocytes. *Cell Mol Life Sci*, **60**, 1504-1512.
- 35 Yu, Y.H., Liao, P.R., Guo, C.J., Chen, C.H., Mochly-Rosen, D. and Chuang, L.M. (2016) PKC-ALDH2 Pathway Plays a Novel Role in Adipocyte Differentiation. *PLoS One*, **11**, e0161993.
- 36 Chen, W.S., Xu, P.Z., Gottlob, K., Chen, M.L., Sokol, K., Shiyanova, T., Roninson, I., Weng, W., Suzuki, R., Tobe, K. *et al.* (2001) Growth retardation and increased apoptosis in mice with homozygous disruption of the Akt1 gene. *Genes Dev*, **15**, 2203-2208.
- 37 Peng, X.D., Xu, P.Z., Chen, M.L., Hahn-Windgassen, A., Skeen, J., Jacobs, J., Sundararajan, D., Chen, W.S., Crawford, S.E., Coleman, K.G. *et al.* (2003) Dwarfism, impaired skin development, skeletal muscle atrophy, delayed bone development, and impeded adipogenesis in mice lacking Akt1 and Akt2. *Genes Dev*, **17**, 1352-1365.
- 38 Winnay, J.N., Solheim, M.H., Dirice, E., Sakaguchi, M., Noh, H.L., Kang, H.J., Takahashi, H., Chudasama, K.K., Kim, J.K., Molven, A. *et al.* (2016) PI3-kinase mutation linked to insulin and growth factor resistance in vivo. *J Clin Invest*, **126**, 1401-1412.
- 39 Li, H. and Durbin, R. (2010) Fast and accurate long-read alignment with Burrows-Wheeler transform. *Bioinformatics*, **26**, 589-595.
- 40 McKenna, A., Hanna, M., Banks, E., Sivachenko, A., Cibulskis, K., Kernytsky, A., Garimella, K., Altshuler, D., Gabriel, S., Daly, M. *et al.* (2010) The Genome Analysis Toolkit: a MapReduce framework for analyzing next-generation DNA sequencing data. *Genome Res*, **20**, 1297-1303.

Figure Legends

Figure 1

Photographs of the individual with PKC ϵ -SHORT syndrome. **A-B** show the individual as a newborn. At birth she was noted to have a prominent nasal bridge and nose with a small chin. **C** shows the individual in infancy. She had a sparseness of hair, a broad forehead, deep set eyes, small chin, and prominent varicosities. **D-E** shows the individual as an adolescent. Her face is triangular in appearance, palpebral fissures were deep set and she continued to have a prominent nasal root. Her nose was long, narrow with an overhanging columella and small alae nasi. Ears were prominent, and hair texture was thin.

Figure 2

A. Primary structure of PKC ϵ showing the position of the Ser/Thr kinase catalytic domain relative to other important functional regions that constitute the regulatory domain including C2; conventional PKC domain [Ca²⁺] binding region, PS; pseudosubstrate autoinhibitory domain, C1A; actin-binding domain, C1B; PMA and diacyl glycerol (DAG)-induced membrane binding domain. Priming phosphorylation residues include Thr566 (activation loop motif), Thr710 (turn motif) and Ser729 (hydrophobic motif). A159E is a constitutively active (CA) variant and K437M an ATP-binding defective kinase-dead variant. The patient mutation E599K is indicated in grey. E599 is invariantly conserved amongst multiple different species (Supplementary Table 2).

B. The left hand panel depicts a schematic showing how the non-radioactive fluorescent PKC-specific peptide substrate phosphorylation is resolved by agarose gel electrophoresis based on its net charge ("P" indicates phosphorylation). The middle panel shows a representative agarose gel showing the kinetics of PKC ϵ -dependent phosphorylation of the PKC reporter Phospho-PepTag peptide up to 45mins. Wild-type (WT), E599K and K437 (KD; kinase-dead) PKC ϵ expressed and immunoprecipitated from HEK293 cells was assessed for kinase activity using this system. Recombinant PKC (recPKC) supplied with the

assay kit served as a positive control. Reduced phospho-peptide substrate levels are observed in E599K and K437M compared to WT and recPKC. The western blot panel below shows equivalent expression of wild-type (WT) and E599K PKC ϵ used in the kinase activity analysis.

C. E599K kinase activity is approximately 50% less than that of wild-type (WT). The plot depicts a quantitation of the phospho-PepTag peptide signal at 45min time point normalised to WT. Error bars represent the mean \pm S.D. (n=3) (* $P < 0.05$ Student's t test).

D. Equal amounts (5 μ l each) of wild-type (WT) and E599K were mixed together and assessed for kinase activity. Interestingly, additivity was not observed, suggesting E599K may also exhibit a degree of dominant negativity (NS; not significant by Student's t test).

Figure 3

A. PKC ϵ along with all AGC kinase family members require phosphorylation of specific priming sites for optimal activity. For PKC ϵ the priming kinases include PDK1 and mTORC2 complex. Primed kinase exists in equilibrium between an autoinhibited latent kinase and a fully active kinase. A dynamic allosteric conformational change within the catalytic kinase domain upon substrate and ATP binding is required for full enzymatic activation.

B. Priming phosphorylation on PKC ϵ -S729 was determined using extracts derived from parental and patient LCLs. Titration analysis indicates that pPKC ϵ -S729 were reduced in PKC ϵ SHORT syndrome LCLs compared to parental LCLs.

C. PKC ϵ from PKC ϵ SHORT syndrome LCLs displayed enhanced affinity for the mTORC2 subunit SIN1 compared to that from parental LCLs. Endogenous SIN1 was immunoprecipitated from LCLs and probed for PKC ϵ and SIN1, as indicated.

D. PKC ϵ E599K binds with increased affinity to SIN1 compared to wild-type (WT). Constructs were ectopically expressed in HEK293 cells, immunoprecipitated using FLAG-beads (IP) and western blotted with anti-SIN1. Differing exposures are shown.

E. PKC ϵ E599K binds to PDK1 with comparable affinity as wild-type (WT) PKC ϵ . Constructs were ectopically expressed in HEK293 cells, immunoprecipitated using FLAG-beads (IP) and western blotted with anti-PDK1. Differing exposures are shown.

F. Priming phosphorylation on PKC ϵ -S729 was determined on FLAG-immunoprecipitated wild-type (WT) and E599K PKC ϵ following ectopic expression in HEK293 cells. Under these conditions equal levels of pPKC ϵ -S729 were observed.

G. Indicated constructs were ectopically expressed in HEK293 cells, immunoprecipitated using FLAG-beads probed using anti-pPKC ϵ -S729 and anti-FLAG. Unt; untransfected, WT; wild-type PKC ϵ , CA; constitutionally active PKC ϵ , KD; kinase-dead, and E599K; SHORT syndrome patient variant.

H. PKC ϵ E599K exhibits altered dynamic flexibility in priming S729. As in D, E and G, constructs were ectopically expressed in HEK293 cells, immunoprecipitated using FLAG-beads probed using anti-pPKC ϵ -S729 and anti-FLAG. KD; this refers to K437M ATP binding defective kinase-dead variant that strips PKC ϵ of its priming phosphorylations. KD + CA; K473M together *in cis* with the constitutively active A159E. Here, priming on S729 is also significantly reduced. KD + E599K; the patient mutation (E599K) together *in cis* with the kinase-dead K473M. Here, priming on S729 is clearly detectable and demonstrates an inflexibility in allosteric dynamics in PKC ϵ induced by E599K.

Figure 4

A. Rapamycin inhibits mTORC1 complex specifically but can be used to monitor mTORC2 complex activity. LCLs from an unaffected parent and from the PKC ϵ SHORT syndrome individual were treated with 200nM rapamycin (RapM) as indicated and probed using specific anti-sera for mTORC2 and PDK1-dependent priming phosphorylations on AKT. PKC ϵ SHORT syndrome LCLs selectively exhibited attenuated mTORC2-dependent pAKT-S473 under these conditions, compared to parental LCLs. By contrast, the kinetics of PDK1-dependent pAKT-T308 were unaffected between patient and control LCLs. Nonetheless, for optimal activity, AKT must be phosphorylated on both these priming residues. Consequently, reduced pFOXO1-S256 was also observed in PKC ϵ SHORT syndrome LCLs following RapM, compared to wild-type LCLs (WT).

B. Wild-type (WT) and p85 α -SHORT syndrome LCLs (*PIK3R1*; p.N636Tfs*18) were treated as in B. Here, p85 α -SHORT syndrome LCLs exhibited markedly reduced PDK1-dependent pAKT-T308. Reduced AKT-dependent pFOXO1-S256 was also evident under these conditions.

C. HEK293 cells were transfected as indicated and treated with 200nM rapamycin (RapM) and assessed for mTORC2-dependent priming phosphorylation of AKT on S473. E599K SHORT syndrome patient mutation and the kinase-dead (KD) K473M both exhibited reduced AKT priming under these conditions, in contrast to wild-type (WT) PKC ϵ .

D. LCLs were grown in low serum conditions (LS; 0.5% FCS for 24hrs) before treatment with 5 μ M PMA as indicated. AKT-mTOR pathway activity was indirectly assessed using S6 phosphorylation on S240 and S244. Whilst PMA failed to dramatically impact upon pS6-S240/244 levels in parental LCLs under these conditions, by contrast, PKC ϵ SHORT syndrome LCLs clearly showed reduced pS6-S240/244 reflective of reduced AKT-mTOR pathway activity

Figure 5

A simplified schematic demonstrating the key nodes of the PI3K-AKT-mTOR signaling network and how these are altered in SHORT syndrome that is ultimately associated with reduced signal transduction through this pathway. Impaired signal transduction is noted by the dashed lines. The left-hand schematic shows the situation in SHORT syndrome caused by dominant *de novo* variants in *PIK3R1* which encodes the p85 α regulatory subunit of PI3K. Here, the predominant abnormality is reduced PDK1-dependent priming of AKT by phosphorylation at T308. It is likely that PDK1-dependent priming of PKC ϵ may also be compromised under these circumstances but we have not investigated this. The right-hand schematic depicts the situation in SHORT syndrome caused by the dominant *de novo* E599K mutation of *PRKCE* (PKC ϵ) identified and characterized in this study. Here we showed that expression of this variant causes reduced mTORC2-dependent priming of AKT by phosphorylation at S473. SIN1 is highlighted here (mTORC2 is a multicomponent complex), because of the interaction works shown in Figure 3. Enhanced affinity of E599K for SIN1 could disproportionately negatively impact AKT activation, by leaving a reduced pool of SIN1-mTORC2 available to prime AKT. Importantly, AKT needs to be phosphorylated on both these priming sites (along with its turn motif residue T450) for optimal kinase activity and effective signaling from AKT to mTOR and further downstream. Furthermore, impacting upon the positive feedback loop between AKT and mTORC2 via SIN1 phosphorylation by AKT could also attenuate signaling flux. In summary, PKC ϵ SHORT syndrome, similar to p85 α -SHORT syndrome, exhibits reduced AKT-mTOR activity at the level of AKT phospho-priming. In the case of the latter this is predominantly via the PDK1 route, whilst in the former it appears to be via the mTORC2 route.



Figure 1.

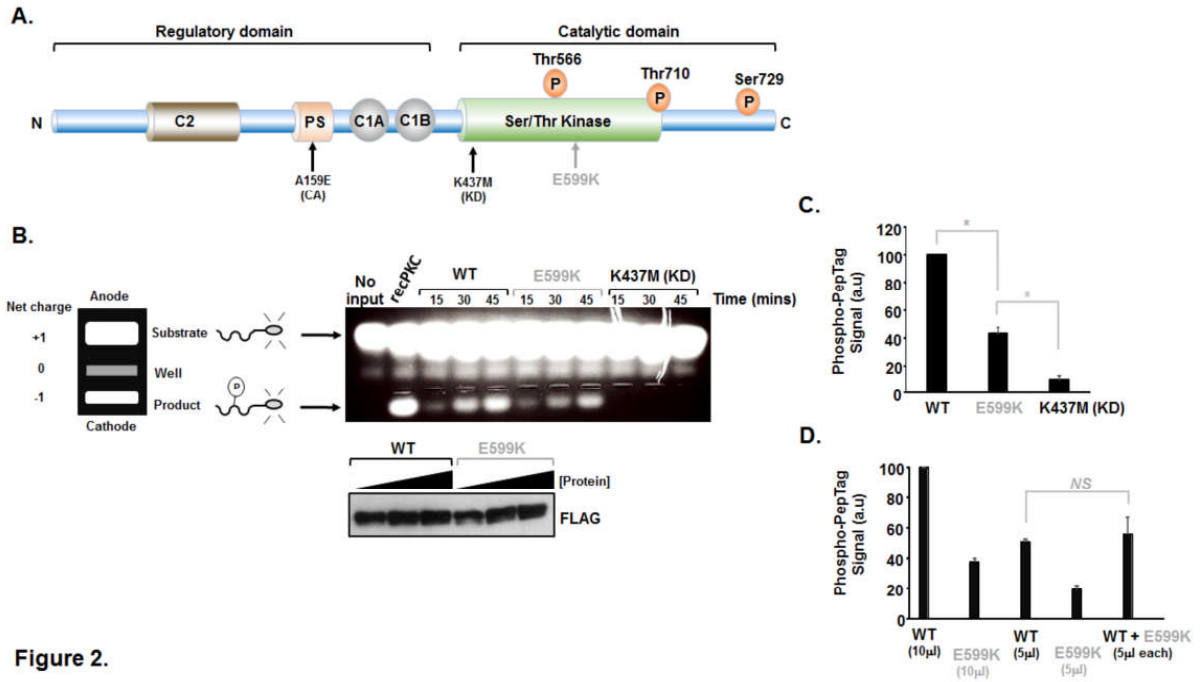


Figure 2.

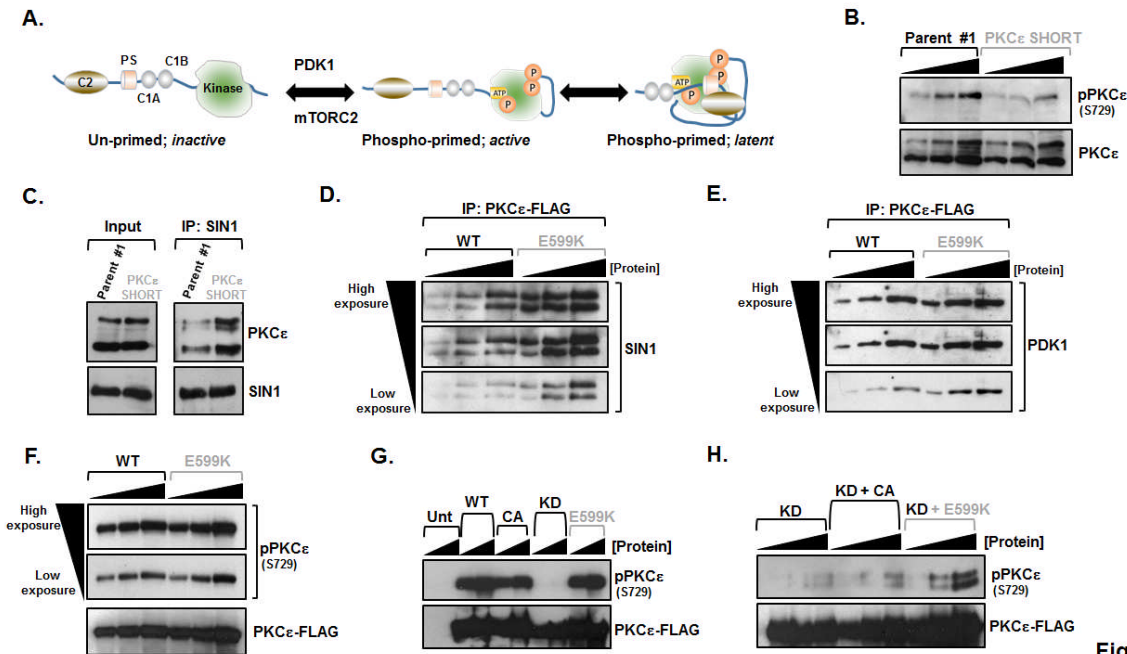


Figure 3.

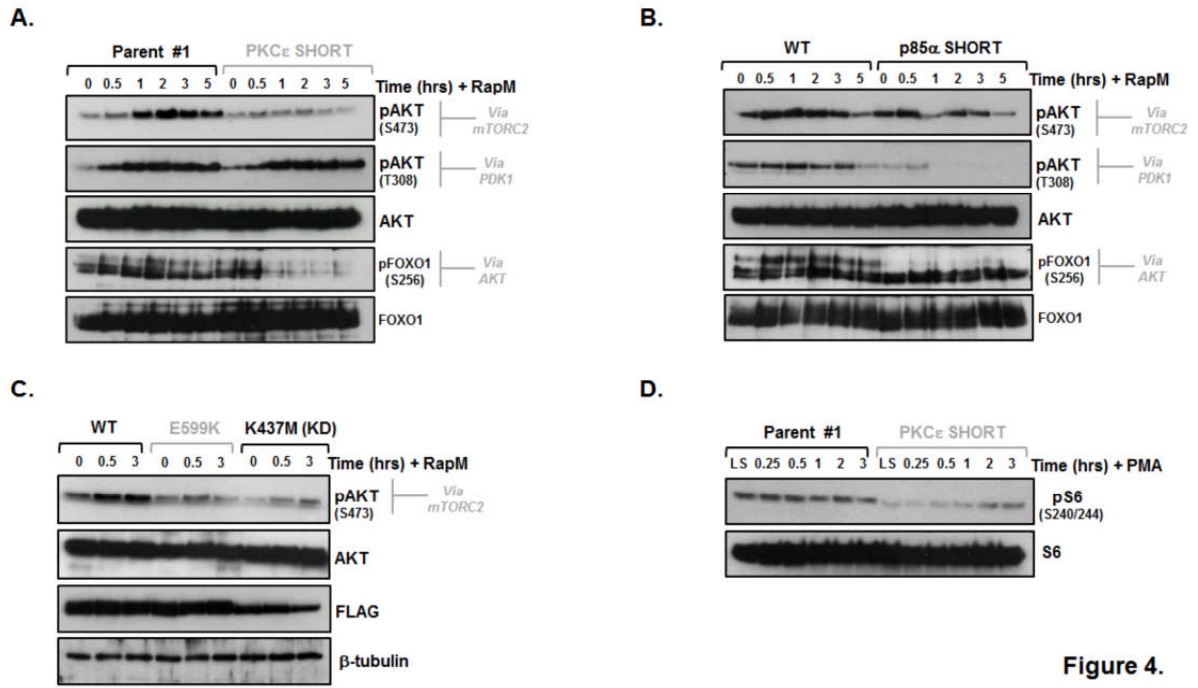


Figure 4.

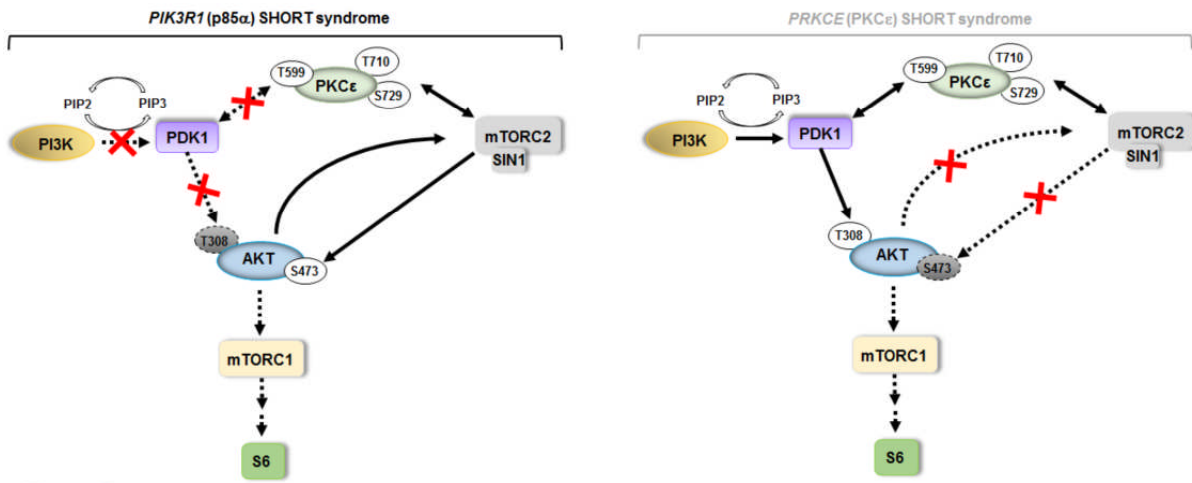


Figure 5.